Environ. Eng. Res. 2016; 21(1): 1-14
http://dx.doi.org/10.4491/eer.2015.086

pISSN 1226-1025
eISSN 2005-968X

Flocculation kinetics and hydrodynamic interactions in natural and engineered flow systems: A review

Benjamin Oyegbile[1†], Peter Ay[2], Satyanarayana Narra[1,2]

[1]*Chair of Minerals Processing, Brandenburgische Technische Universität Cottbus-Senftenberg, Cottbus 03046, Germany*
[2]*Department of Technical Environment and Climate Protection, Lübeck University of Applied Sciences, Lübeck 23562, Germany*

ABSTRACT

Flocculation is a widely used phase separation technique in industrial unit processes and is typically observed in many natural flow systems. Advances in colloidal chemistry over the past decades has vastly improved our understanding of this phenomenon. However, in many practical applications, process engineering still lags developments in colloidal science thereby creating a gap in knowledge. While significant progress has been made in environmental process engineering research over the past decades, there is still a need to align these two inter-dependent fields of research more closely. This paper provides a comprehensive review of the flocculation mechanism from empirical and theoretical perspective, discuss its practical applications, and examines the need and direction of future research.

Keywords: Floc stability, Hydrodynamics, Orthokinetic, Pelleting flocculation, Turbulence

1. Introduction

In environmental management, the removal of particulate solids from liquid process effluents is of great importance. However, when the sizes of solid particles diminish and reach micron and submicron range, the particles tend to remain in suspension and cannot be removed by gravity settling. In order to achieve an acceptable solid-liquid separation at a reasonable cost, the particles need to be agglomerated by flocculation followed by phase separation (sedimentation, filtration, centrifugation etc.) [1]

Flocculation plays a key role in several natural processes in the aquatic and marine environment such as sediment erosion, transport, aggregation and deposition and it is often employed in several industrial purification and separation processes [2-8]. Aggregation of cohesive suspended particles by size enlargement to form larger flocs is typically encountered in natural systems such as rivers, reservoirs, lakes and estuarine and in engineered systems such as bioreactors and agitation vessels [9-13]. It is widely employed in both upstream and downstream solid-liquid separation processes where the value of the individual phases are enhanced by destabilization and aggregation of the charged particles in suspension using high molecular weight synthetic polymers [14-18].

Typical mean shear rates in these diverse natural and engineered systems range from 2.5/s in natural systems to 5000/s especially in high shear bioreactors and mixing chambers [19, 20]. A number of interfacial forces and interactions that play key roles in this process are well-understood in the light of classical and extended DLVO theory [21-25], and provides a basis for any theoretical analysis of particle dispersion and colloidal stability. Therefore, the aim of this review paper is to provide an insight into the role of colloidal physicochemical process and hydrodynamics interactions in particle aggregation process—floc aggregation, growth and stability, and summarize the recent contributions in this field to the understanding of turbulence phenomenon and the direction of future research.

2. Structure Formation Processes in Dispersed Systems

2.1. Colloidal Stability and Interfacial Forces

Most colloidal particles in suspension (0.001 - 10 μm) tend to remain suspended and settle very slowly due to the presence of surface charge arising from isomorphic substitution, chemical reaction at the interface or preferential adsorption of ions on the particle surface from the surrounding medium [26, 27]. The charge on the particle surface is surrounded by excess of oppositely charged ions (counterions) in solution in order to maintain electrical

Received August 1, 2015 **Accepted** March 3, 2016

† Corresponding author
Email: oyegbaki@tu-cottbus.de
Tel: +49 (0)355-69-4324 Fax: +49 (0)355-69-2929

neutrality. The combined interactions of this system of opposite charged cloud is known as the electric double layer [28]. The developed electrostatic repulsive forces prevent particle aggregation in colloidal system and hence contribute to their stability in the dispersed system [29]. The diffuse layer and the Stern layer of the charge cloud surrounding a particle together constitute the electric double layer [30].

A quantitative description of the colloidal stability and aggregation process was facilitated by the assumptions of the DLVO theory which considered interactions between particles as additive [28]. The DLVO theory was primarily based on two types of interactions between two compact spherical particles—electrostatic (including *Born repulsion*) [31] repulsive force due to the electrical double layer and Van der Waals attractive force of the dispersion.

The combination of these two interactions defines a total energy barrier V_T or the so-called *Gibbs interaction energy* as shown in the energy profile in Fig. 1 [32, 28, 33-35, 25] which, if overcome by the kinetic energy of the moving particles, will result in aggregation. This is expressed mathematically in Eqs. (1-2), where V_A, V_R, ζ refers to the energy barrier due to Van der Waals attraction and electrostatic repulsion and zeta potential respectively. In the case of submicron particles, the kinetic energy is derived primarily from Brownian diffusion and less from hydrodynamic (fluid shear) or gravitational forces (differential settling). However, for larger or coarser particles, hydrodynamic interactions such as turbulence or fluid shear and gravitational forces imparts much of the kinetic energy needed to overcome the flocculation barrier [36, 33, 37]. A critical shear rate is required to overcome the energy barrier in order to allow flocculation and floc formation, and this is dependent on the surface charge and the size of particles. In general, the higher the charge on the particles, and the smaller the particle size, the higher the shear rates that are required to bring about flocculation [21, 35, 38].

$$V_T = V_R + V_A \tag{1}$$

$$V_T = \pi\epsilon\zeta^2 dexp(-kh) - \frac{Ad}{24h} \tag{2}$$

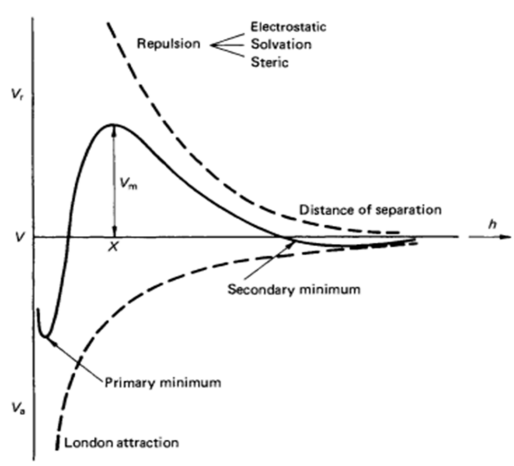

Fig. 1. Potential energy barrier in the interaction between two particles [37] © 1993 Elsevier.

In addition to the interactions described above, there exist additional interaction energies and structural forces which may arise for instance from the perturbation or re-arrangement of water molecules near the interface [4, 34, 39]. Non-DLVO interactions such as hydrophobic, hydration, oscillatory, structural, steric and electrosteric and hydrodynamic forces, which were previously not considered in colloidal interactions are now widely recognized to play important roles in colloidal aggregation [4, 21, 40-42]. These forces may be attractive, repulsive or oscillatory in nature and may be more pronounced or stronger than the DLVO forces [4]. In some cases where the energy barrier for aggregation exists at subnanometer distances, significant discrepancies between theoretical (DLVO-based) and experimental measurements of flocculation rates have been reported [13, 36]. For instance, in the case of colloidal dispersion containing clay particles, the theory provides a general conceptual model for the gross interactions of particles but fails to explain certain aspects of the interactions [27]. However, in most practical applications of flocculation, the dominant forces are electrostatic repulsion and London-Van der Waals attraction forces [43].

2.2. Kinetics of Fine Particle Aggregation

Flocculation kinetics deal with time-dependent changes in the dispersions or suspensions and provides information on the flocculation rate, dispersion stability and particle interactions which depends on the number and efficiency of the collisions [44]. The collisions between particles has been suggested to occur at a rate that depends on the transport mechanisms of Brownian diffusion, fluid shear and differential settling and it is assumed to be a second-order rate or reaction process [45]. The aggregation of dilute systems (TS ≤ 1%) with an initial concentration of primary particles n1 and fast aggregation constant k^f can be represented by the expression in Eq. (3) [31, 45].

$$\frac{dn_1}{dt} = -k^f n_1^2 \tag{3}$$

Furthermore, several studies have shown that aggregates formed from different transport mechanisms exhibit marked variations in their structural attributes. The aggregates formed by shear-induced collision are known to be stronger than those formed from other transport mechanisms, those from Brownian motion tend to be easily dispersed by shearing, while those from differential settling results in ragged, weak, and low density aggregates [46].

Smoluchowski using the "population balance" approach, expressed time evolution of the number density of discrete particles of size k as they aggregate with respect to time in terms of the collision frequency or rate function β originally for Brownian diffusion and laminar or uniform shear flow, and later for differential settling assuming binary collisions between the particles [40, 45, 47-49]. Although the Smoluchowski equation has been modified in line with recent findings to include several other parameters, the general form of the expression is presented in Eq. (4). The quantity β_{ij} is the collision frequency or rate function for collisions between ith and jth sized particles while α_{ij} is the dimensionless collision efficiency factor. The collision frequency depends on the transport mechanisms of Brownian motion, fluid

shear and differential settling, whereas the collision efficiency is a function of the degree of particle destabilization and it gives the probability of collision leading to attachment with values ranging from 0 to 1 [47, 50-53].

$$\frac{dn_k}{dt}=\frac{1}{2}\sum_{i+j=k}\beta(i,j)n_i n_j-\sum_{i=1}^{\infty}\beta(i,k)n_i n_k \tag{4}$$

The first term of the right hand side of Eq. 4 describes the increase in number of particles of size k by flocculation of two particles whose total volume is equal to the volume of a particle of size k, while the second term on the right hand side describes the loss of particles of size k due to aggregation with particles of other sizes. The general form of the equation expresses the rate of change in the number concentration of particles of size k. In arriving at Eq. (4), Smoluchowski made a number of key assumptions listed below:

- The collision efficiency factor α is unity for all collisions
- The fluid motion undergoes laminar shear
- The particles are mono dispersed
- There is no breakage of flocs
- All particles are spherical in shape before and after collision
- Collision involves only two particles

2.3. Flocculation Transport Processes

The interparticle collisions are promoted by transport mechanisms of Brownian motion or perikinetic (for particles with diameters less than 1 μm), fluid shear or orthokinetic (for particles in the diameter range 1-40 μm) and differential settling (typically for particles with diameter larger than 40 μm). The collision frequency or rate function β for these three mechanisms can be expressed mathematically in Eqs. (5-7) where β_{BM}, β_{SH}, β_{DS} refers to the collision frequency function for Brownian motion, fluid shear, and differential settling respectively. The total collision rate or frequency β_T is the sum of contributions from each of the three transport mechanisms (Eq. (8)) [3, 5, 10, 46, 48, 51, 54-56].

$$\beta_{BM}=\frac{2kTd_{ij}^2}{3\mu d_i d_j} \tag{5}$$

$$\beta_{SH}=\frac{(d_i+d_{j)}^3}{6}G \tag{6}$$

$$\beta_{DS}=\frac{\pi g}{72v_w}(d_i+d_j)^2(\triangle\rho_i d_i^2-\triangle\rho_j d_j^2) \tag{7}$$

$$\beta_T=\beta_{BM}+\beta_{SH}+\beta_{DS} \tag{8}$$

2.3.1. Perikinetic particle aggregation

The random displacement of particles in Brownian motion as a result of the thermal energy of the system is termed perikinetic [21, 40, 42, 45]. In practical applications, perikinetic aggregation is only important for very small particles where they are continuously bombarded by the surrounding water molecules (< 1 μm) [57]. Under this prevailing condition, the rate of floc growth cannot be sufficiently sustained for an effective phase separation. Hence, the importance of other transport mechanisms in promoting the floc growth kinetics. However, in the case of contact between a small particle and micro flocs, Brownian diffusion can still control the transport of small particles across the layer of fluid on the floc surface [58].

2.3.2. Classical orthokinetic aggregation

The agitation of suspended particles in liquid medium will lead to aggregation due to the inter particle collision induced by the fluid motion [37]. The velocity gradient or shear rate is dependent on the nature of the fluid flow. In uniform laminar shear flow, the velocity gradient remains constant in the entire flow field while in turbulent flow, there is a rapid fluctuation of the velocity gradient. Consequently, the velocity gradient is a function of both space and time (*spatial and temporal*) [59, 60]. Camp and Stein in their critique of the Smoluchowski approach to shear flocculation modelling [61], introduced the concept of root-mean-square (R.M.S.) or absolute velocity gradient $\overline{G}$ to account for the variations in the shear rate. [26, 46, 58, 62, 63]. Considering the angular distortion of an elemental volume of fluid arising from the application of tangential surface forces, $\overline{G}$ is defined according to Eqs. (9-10) as the R.M.S. velocity gradient in the mixing vessel, where u, v, w are the components of the fluctuating velocity while x, y, z refers to the 3-D Cartesian coordinate system, P is the power dissipated, V is the volume of the mixing vessel, ϵ is the energy dissipation rate per unit mass, μ is the dynamic viscosity and v is the kinematic viscosity [26, 64].

$$G=\left\{\left(\frac{\partial u}{\partial y}+\frac{\partial v}{\partial x}\right)^2\left(\frac{\partial u}{\partial z}+\frac{\partial w}{\partial z}\right)^2\left(\frac{\partial v}{\partial z}+\frac{\partial w}{\partial y}\right)^2\right\}^{\frac{1}{2}} \tag{9}$$

$$G=\frac{1}{\tau_{Kolmogorov}}=\sqrt{\frac{p}{\mu V}}=\sqrt{\frac{\epsilon}{v}} \tag{10}$$

In practical applications, owing to the difficulties associated with the calculation of absolute velocity gradient $\overline{G}$ due to the fluctuations in the energy dissipation within the mixing vessel, an average velocity gradient G_{ave} has often been used in place of the absolute value $\overline{G}$ [59, 60] (Eq. (11)). Korpijarvi et. al. [65], in their study of mixing and flocculation in a jar using computational fluid dynamics (CFD) reported a large variation in the local velocity gradient G_L within the mixing vessel. In similar studies conducted by Kramer and Clark [26, 66] as well as Mühle [67], a lower estimate of the absolute velocity gradient was proposed (Eqs. (12-13)) to account for the variation of the velocity gradient throughout the fluid where quantities G_L, P_{ave}, ϵ, V, μ, v represent the local velocity gradient at different points within the mixing vessel, average power consumption, volume of the mixing vessel, kinetic energy dissipation rate, dynamic and kinematic viscosity respectively.

$$G_{ave}=\sqrt{\frac{P_{ave}}{\mu V}}=\sqrt{\frac{\epsilon_{ave}}{v}} \tag{11}$$

$$\overline{G} = \sqrt{\frac{P}{\mu V} - \sigma_{GL}^2} \tag{12}$$

$$\overline{G} = 0.26\sqrt{\frac{P}{V\mu}} = 0.26\sqrt{\frac{\epsilon}{v}} \tag{13}$$

2.3.1.1. Particles in laminar shear

According to the rectilinear model of particle trajectory, two particles moving in a fluid on different streamlines will experience a velocity gradient which indicates the relative motion of particles and the possibility of collision and aggregation [45, 68]. In simple laminar or uniform shear with a well-defined flow field such as in pipe flow or in some Couette devices [19, 69, 70], the transport of particles by laminar shear due to the fluid motion can be characterized by a single value of the shear rate G [26]. Under such condition, the particles in laminar shear will exhibit rotational motion in the direction of travel with a constant angular velocity ω [71, 72].

2.3.1.2. Particles in turbulent shear

In most practical applications of flocculation, the aggregation processes typically occur under turbulent conditions [26, 68, 73-75]. The particles in suspension under the influence of turbulent flow will experience fluctuating motion of the fluid with the particles being transported by the fluid eddies and the flow vortex [26, 58]. Thus, small particles suspended in fluid exist in an environment of small energy-dissipating eddies in most typical sheared reactors [19, 76]. Under such condition, particle collisions are promoted by eddy size similar to that of the colliding particles [47, 77]. The mechanism of flocculation in turbulent shear has been suggested to be similar to that of laminar shear for particles smaller than the Kolmogorov microscale λ_0 of turbulence, while for particle larger than this length scale, the flocculation mechanism is similar to that of Brownian diffusion [21, 26].

The formation of aggregates in any turbulence or shear-induced flocculation essentially consist of the following phases: destabilization; collision and adhesion; floc growth and deformation phases [78]. Ives [69] and Bergenstahl [79] expressed the kinetics of orthokinetic aggregation in terms of the change in the initial particle concentration, while Levich [62, 80] in an earlier study derived the collision rate equation based on the concept of locally isotropic turbulence assuming a viscous diffusive subrange (i.e. particle size smaller than Kolmogorov micro scale) for shear-induced turbulent flow where N, r, d represent the particle number concentration per unit volume, particle radius and diameter respectively (Eqs. (14-15)). Several other models of flocculation kinetics are available in literature [27, 81]. In most of these models, the shear rate G and the kinetic energy dissipation rate ε are shown as important drivers of the flocculation process. Typically, orthokinetic flocculation can be experimentally observed in a conventional stirred tank consisting of an axially mounted impeller and a circular or rectangular mixing vessel.

$$\frac{-dN}{dt_{(Couette)}} = \frac{2}{3} f_o G d^3 N^2 + \frac{4}{3} f_p \frac{kTN^2}{\mu} \tag{14}$$

$$\frac{dN}{dt_{turb.}} = -6\pi\beta\sqrt{\frac{\epsilon_{intensity}}{\eta}}\, r^3 N^2 = -12\pi\beta\sqrt{\frac{\epsilon_{intensity}}{\eta}}\, d^3 N^2 \tag{15}$$

2.3.2. Extended orthokinetic aggregation

Pelleting flocculation is considered as an extension of the classical orthokinetic transport mechanism based on the "metastable state" concept [82, 83]. It has been shown by several studies that the efficiency of the floc formation process as well as the floc structural attributes (size, shape, porosity, density, etc.) can be significantly improved by the application of suitable mechanical energy [84-94]. This is accomplished by the application of a non-destructive uneven force system on the floc surface, by the action of the turbulent fluid motion or the so-called floccule mechanical synaeresis induced by rolling and collision mechanisms [95-99].

In the rolling mechanism, as the floc rolls along a plane surface, it is subjected to a pressure fluctuation which becomes greater at the front of the central point in the contact area and lesser at the rear. On the other hand, in the collision mechanisms, a floc experiences an impact due to the floc-floc or floc-surface collision. In order to withstand this impact, the floc must adhere strongly, in order words, the impact results in a more compact floc [83]. The resulting pressure induced in a curvilinear trajectory on the floc surface can be expressed as a function of the velocity gradient G where m, R, G and A represent the mass of the floc, radius of the flow trajectory, velocity gradient and the area of the floc projection onto a plane oriented normally to the vector of the resultant force respectively (Eq. (16)). In practice, pelleting flocculation is realized through the selection of an appropriate process engineering conditions and stirrer-vessel system (geometry and configuration) in order to obtain the necessary conditions suitable for rolling and collision-mediated floc pelletization. [83, 91].

$$P = \frac{mRG^2}{A} = \frac{mRv^2}{A\lambda_0^4} \tag{16}$$

The structure formation by pelleting flocculation yields "pellet flocs" with superior structural attributes when compared to the "random flocs" produced by the classical flocculation process which tend to be loose and bulky [84]. Previous studies have reported two distinct models of pelleting flocculation, namely parallel and series models resulting in onion and raspberry-like pellet floc structures as presented schematically in Fig. 2 [87, 90, 91, 100-103]. In the series model, orthokinetic flocculation occurs first where random, loose and bulky flocs are produced. These voluminous flocs shrink and densify by the application of suitable mechanical energy (mechanical synaeresis).

Conversely, in the parallel model, there is no time delay between the orthokinetic flocculation and mechanical synaeresis. The dispersed particles in suspension and micro flocs are transported by the fluid motion to the surface of the "mother seed" where they are attached by polymer bridging [95, 100, 102]. In terms of the flocculation efficiency and process relevant (phase separation) parameters, pellet flocs can be characterized by their size, shape, density, porosity, compressive strength and deformability.

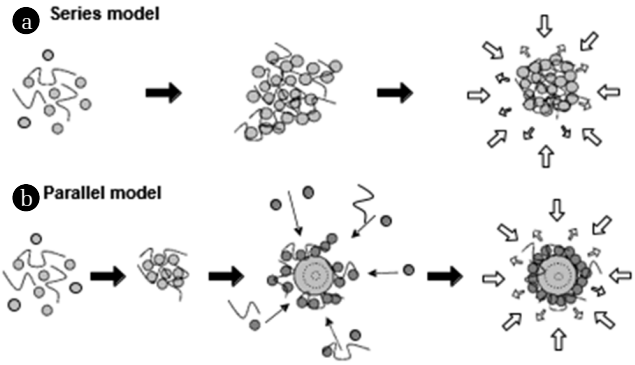

Fig. 2. Conceptual models of pelleting flocculation process (a) series model: raspberry structure (b) parallel model: onion structure.

2.3.3. Polymer-mediated interactions

The energy barrier to flocculation can be overcome in several other ways apart from the kinetic energy derived from the transport mechanisms. The electrostatic charge can be lowered with the aid of polymeric flocculants by double layer compression, charge neutralization, and polymer bridging between particles [32, 33, 104]. In practice, both of these approaches are employed either concurrently or sequentially. In addition to these interactions, several other mechanisms have also been attributed to the polymer flocculation of charged particles in suspension. Electrostatic charge-patch; depletion flocculation; network flocculation and polymer complex formation are few of the other relevant interactions [2, 4, 36, 38, 73, 105-108].

However, the dominant concepts in the case of polyelectrolyte-mediated destabilization are surface charge neutralization (ion exchange), charge patch formation and polymer bridging as illustrated in Fig. 3 [44, 109-115]. The important physicochemical properties that influence the flocculation process in the case of polymer-mediated interactions include, polymer molecular weight, charge density and concentration, zeta potential or surface charge of suspension, particle size and distribution, specific surface area, solution conductivity and pH [105].

In the case of pelleting flocculation, Higashitani and Kubota [98] in their study of the pelleting flocculation of polystyrene latex particles reported that the formation of pellet flocs depends on the suspension concentration, flocculant molecular weight and charge density as well as the intensity of mixing. They argued that pellet flocs are formed within a limited range of these parameters hence pelleting flocculation requires a high degree of control of different process conditions. On the basis of their findings, they expressed mathematically the volume fraction of particles $\varnothing_{pt}$ at the critical particle concentration N_c above which pellet flocs are formed as a function of the initial particle concentration N_0, polymer concentration C_p, charge density p, and the molecular weight M, where N_A is the Avogadro constant (Eq. (17)).

$$\varnothing_{pt} = 4\times10^{-5}\frac{C_p N_A}{pN_0 M} = 24.08\times10^{18}\frac{C_p}{pN_0 M} \qquad (17)$$

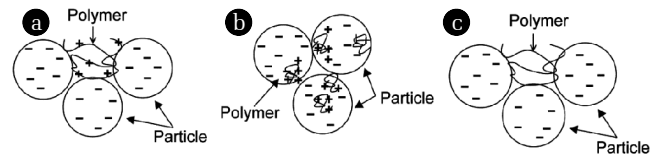

Fig. 3. A schematic representation of the dominant mechanisms in polymer-mediated interactions (a) charge neutralization (b) charge patch formation (c) polymer bridging.

3. Hydrodynamics of Fine Particle Aggregation

Hydrodynamically-induced turbulent shear is an important driver of the flocculation process especially in the case of *orthokinetic* aggregation of particles [33, 36, 116]. The floc growth and stability in any flocculated system has been suggested to be a function fluid-particle interactions and the intrinsic physicochemical properties of the floc [75, 77, 117]. The dynamics of these interactions affects all facets of the flocculation process and the degree of aggregation in any sheared system [118]. In the case of hydrodynamic interactions, induced velocity gradient promote the aggregation process but might also be responsible for floc breakage as a result of increased viscous shear stress [119]. Consequently, in the case of shear-induced collisions, the hydrodynamic effect can be very significant [57].

The chemical transport in natural and engineered systems is often controlled more by the fluid properties, in this case the mixing rate of the fluid, than by chemical properties such as the molecular diffusivity of the compound. Therefore, in the design of flocculation reactors, it is desirable to have uniform mixing intensities throughout the reactor [26]. Under the condition of shear-induced turbulence due to the use of flow inducers such as paddles, mixers, stirrers or bubbles (Fig. 4), the convective currents in the system are insignificant as compared to the advective currents generated in the system [19]. The numerical modelling of the phenomena of fluid-particle mixing, floc formation, growth and breakup is very complex, as such minimizing the energy dissipation rate (degree of turbulent mixing) in the reactor will lead to improvement in flocculation efficiency [26].

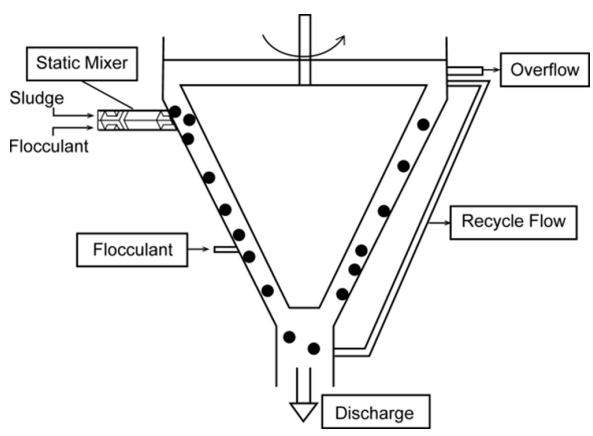

Fig. 4. Schematic diagram of a pelleting reactor showing the role of mixing in the structure formation process.

3.1. Fluid Mixing and Particle Dispersion

Turbulent mixing characterized by high Reynolds number ($R^e > 10^4$) [120], can be viewed as a hierarchy of irregular, rotational and dissipative motion containing vorticity (curl or rotation of the velocity vector) on different scales or eddy sizes [25, 121]. In turbulent flows such as those encountered in pipe or tube flow, channel flow and stirred tanks or mixing chambers, energy transfer occurs on different eddy scales [64, 67]. Eddies are spatial recognizable flow patterns that exist in a turbulent flow for at least a short time in which there is a correlation between the velocities at two different points [26]. Fluid deformation causes vortices to stretch and vorticity and kinetic energy to be transported from larger to smaller eddies [25, 121]. The turbulent vortex in such fluid motion is generally propagated in the tangential and axial direction than in the radial direction with the vorticity increasing with decreasing eddy size [64, 121, 122].

In most practical applications there exist three scales of mixing namely: macro, meso and micro mixing. Macromixing refers to mixing that is driven by the largest scale of motion in the fluid Λ (integral length scale), meso mixing on the other hand involves mixing on a scale smaller than the bulk circulation but larger than the micro mixing, while micro mixing is the mixing on the smallest scale of fluid motion λ_0 (Kolmogorov microscale) expressed in Eq. (18) and at the final scales of molecular diffusivity (Batchelor scale) [120, 123-126]. Micromixing describes the process homogenization of liquid balls with their surroundings on a molecular level. In typical mixing conditions, the dividing line between micro and macro scale is between 100 and 1000 μm respectively [127].

$$\lambda_0 = \left[\frac{v^3}{\epsilon}\right]^{\frac{1}{4}} \tag{18}$$

The largest eddies in turbulent dispersion that represent the macro scale of turbulence or the integral length scale (Λ) contains most of the energy, and are produced by the stirrer or agitator head. The size of this macroscale of turbulence is of the order of the diameter of the agitator [19, 53, 120]. The turbulent flow can be viewed as an eddy continuum, with their size ranging from the dimension of the turbulence generating device to the Kolmogorov length scale [53]. In between the energy-containing eddies of the integral length scale Λ at the upper end of the inertia subrange and the smallest eddies of Kolmogorov microscale λ_0 at the beginning of viscous dissipation range [128], there exist many eddies of other scales smaller than the integral scale Λ that transfer kinetic energy continually through the other length scales. The Batchelor λ_B and Taylor λ_T scales expressed in Eqs. (19-20) are the examples of other important length scales where D is the diameter of the flocs while ϵ is the turbulent kinetic energy dissipation rate.

$$\lambda_B = \left[\frac{D^2 v}{\epsilon}\right]^{\frac{1}{4}} \tag{19}$$

$$\lambda_T = \frac{u\sqrt{15}}{\sqrt{\frac{\epsilon}{v}}} \tag{20}$$

The Taylor scale λ_T is an intermediate length scale in the viscous subrange that is representative of the energy transfer from large to small scales, but it is not a dissipation scale and does not represent any distinct group of eddies [129]. Batchelor micro-scale on the other hand is a limiting length scale where the rate of molecular diffusion is equal to the rate of dissipation of turbulent kinetic energy and represent the size of the region within which a molecule moves due to diffusional forces [123, 125, 128, 130].

3.2. Energy Dissipation in Turbulent Flow

The power input into any agitated system will eventually dissipates as heat due to viscous forces [76]. The larger eddies of the order of the agitator diameter ($\Lambda \sim d_A$) draw energy from the fluid motion, while the smaller eddies transfer that energy gradually and continually to the smallest eddy, where the energy is ultimately dissipated into heat by friction [27]. The turbulence parameters of interest in any agitated micro-system (with respect to the mixer capacity and performance) are the Kolmogorov micro scale λ_0, turbulence kinetic energy dissipation rate ε, and agitator tip velocity V_{tip}[122, 124, 131].

The Kolmogorov length scale λ_0 is an indicator of the rate of micro mixing and mode of agglomerate deformation due to turbulent shear while the energy dissipation rate ε is the rate of the dissipation of kinetic energy. The tip velocity V_{tip} is a measure of the tangential velocity imparted by the flow inducer, an indicator of the strength of the vortex generated by the flow. Peripheral velocity V_{pkol} on the other hand gives an indication of the velocity of the flow vortex at Kolmogorov micro-scale [76, 122, 124, 131]. In typical laboratory mixing experiments (D < 1m), the micro-scale of turbulence predominates. Under such conditions, particle collision is promoted by eddy size similar to those of the colliding particles [47].

4. Floc Stability in Sheared Systems

Floc stability under the influence of hydrodynamic force has been suggested to be a function of floc binding or cohesive force F_B, and hydrodynamic breaking force F_H [64, 81, 116, 132-135]. While the binding force is determined by the flocs' structure and physicochemical attributes, flow turbulence is the principal factor in the case of hydrodynamic force [59, 75, 117]. Of these two governing factors of floc stability, turbulence is the least understood owing to its complex nature [45, 136]. Therefore, a detailed analysis of floc stability under turbulent conditions often encountered in natural and agitated systems is not only difficult but often time consuming [45].

Recent advances in computational fluid dynamics has vastly improved the understanding of turbulence phenomenon. However, numerical modelling of complex turbulent fluid-particle interactions remains a challenge in fluid mechanics and it is computationally intensive [122]. In addition, the assumption of the rectilinear motion of particles prior to collision in flocculation modelling has been supplanted by recent findings of curvi-

linear particle trajectory prior to collisions [47, 63]. Particles have been shown to move around other particles in a curvilinear path thereby reducing the probability of collision and attachment [47, 57].

4.1. Aggregate Strength and Hydrodynamic Stress

Floc formation and growth process in turbulent flocculation comprises of the lag phase, swift growth phase, and steady state phase or breakup/restructuring phase [135, 137, 138]. The overall rate of floc growth at the initial formation phase up to the steady state phase has been suggested to be a balance between collision-induced particle aggregation and floc cohesive strength on one hand, and the rate of floc breakage due to hydrodynamic stress on the other hand [64, 81, 116, 132-134, 139, 140].

The aggregate cohesive strength τ is a function of the physicochemical conditions and floc properties while the turbulent hydrodynamic stress σ depends on the design of the aggregation unit (geometry) and the mixing intensity [27, 75, 81, 117, 132, 134, 141, 142]. A number of empirical models have been proposed for predicting the maximum hydrodynamic breaking force F_H and the global hydrodynamic stress σ acting on a spherical aggregate in the inertia and viscous domain of turbulence (Table. 1).

Table 1. Empirical and Theoretical Models of Maximum Hydrodynamic Breaking Force

Models	Maximum hydrodynamic force	References
1	$F_{Hmax}=\rho\epsilon^{\frac{2}{3}}d_f^{\frac{8}{3}}$	[2, 145][a]
2	$F_{Hmax}=\frac{5}{8}\pi\mu d^2 G$	[140][b]
3	$F_{Hmax}=\frac{5}{8}\rho C_1\epsilon^{\frac{2}{3}}d^{\frac{8}{3}}$	[59, 140]c
4	$F_{Hmax}=\left(\frac{\pi\rho_f\epsilon^{\frac{2}{3}}d^{\frac{8}{3}}}{4}\right)$	[135]c
5	$F_{Hmax}=\frac{\pi\rho\epsilon}{60\mu}d^4$	[135]d
6	$F_{Hmax}=\frac{\rho_{fe}d_f^4}{\mu}$	[145]d
7	$F_{Hmax}=\mu G d_f^2$	[81]
8	$F_{Hmax}=\frac{\pi\mu d_f^2 G}{2}$	[119]
9	$F_{Hmax}=\frac{\pi\sigma d_f^2}{4}$	[64, 146]d
10	$F_{Hmax}=\rho^{\frac{1}{3}}\epsilon^{\frac{2}{3}}d^{\frac{8}{3}}$	[27]c
11	$F_{Hmax}=\frac{\rho\epsilon d_f^4}{\mu}$	[27]d
12	$F_{Hmax}=d_F d_p vG=d_F D_p\sqrt{\epsilon v}$	[67]d

[a]Inertia subrange of turbulence
[b]Viscous subrange of turbulence

He et. al. [135], in a study of floc strength under turbulent flow conditions derived a mathematical expression for an estimate of the floc binding or cohesive force F_B using fractal dimension approach while Lu et al. [35] in a similar study presented a theoretical model for the aggregate binding force F_B of spherical mono-disperse particles both of which are presented in Eq. (21-22). Yuan & Farnood [143], as well as Jarvis et. al. [144], in their review of aggregate strength and breakage gave an estimate of the floc strength τ and global hydrodynamic stress σ obtained from empirical studies of various types of flocs.

$$F_B=48^{-\frac{2}{3}}\pi^{\frac{5}{3}}d^{\frac{2}{3}}\sigma(\rho_o-\rho_w)^{\frac{2}{3}}d^{\left(1+\frac{D_f}{3}\right)} \tag{21}$$

$$F_B=\frac{(1-P_f)F_{Hmax}}{P_f d_p^2} \tag{22}$$

The global hydrodynamic stress σ due to the shearing action of the fluid motion on the floc as well as the overall mechanical strength of an aggregate τ assuming a uniform floc shape and constant porosity can be expressed mathematically in Eqs. (23-24) [77, 116]. In turbulent hydrodynamic flow, the fluctuating motions of the fluid are responsible for shear, tensile, and compressive stress (normal stresses) on the flocs, depending on the direction of the fluctuating velocities acting on the aggregates [67, 77, 147, 148]. The exact type and magnitude of the prevailing stress causing aggregate disruption depends mainly on the relation between the floc size and the eddy size or radius, r_w [67, 149].

$$\sigma=\mu G=\mu\sqrt{\frac{\epsilon}{v}} \tag{23}$$

$$\tau=\frac{(1-p)F_B}{pd_p^2} \tag{24}$$

4.2. Fluid-Particle Interactions and Floc Stability

The size of aggregates varies from molecular dimensions to a range that is visible to the unaided eye, with the smaller sizes being associated with the primary particles of diameter d_p, while the largest size d_{Fmax} is determined by the balance of floc growth and rupture within the fluid [64, 139, 150, 151]. The floc growth and breakage is known to occur simultaneously—growing flocs are subjected to breakage while fragments of broken flocs undergo re-agglomeration until a levelling off of the floc sizes at steady state when the maximum stable size d_{Fmax} is attained [54, 139, 152, 153].

There is an increase in floc size as long as the hydrodynamic force due to turbulent shear is less than the floc cohesive or binding force, and after an extended period of time, an equilibrium floc size distribution is reached. In this case either a continued particle or micro flocs attachment to the larger flocs is prevented, or floc breakup kinetics balances the turbulence-induced collision [27, 67]. Increasing the shear rate (agitation or mixing speed) or

prolonged shearing beyond the steady state leads to a sharp reduction in the mean floc size [10, 27, 35, 139, 154, 155]. The steady-state phase is regarded as the balance between floc growth and breakage under a given shear condition. In the viscous subrange, Lu et. al. [35], expressed this phenomenon in terms of the kinetic equation of flocculation as presented in Eq. (25). The quantities N_A, N_B, σ_S, τ_S, represent change in the particle number concentration per unit volume for aggregation and breakage, the aggregate shear strength and the shearing stress respectively.

$$\frac{dN}{dt} = -\frac{2}{3}\ 0\left(\frac{\epsilon}{v}\right)^{\frac{1}{2}} d_A^3 N_A^2 + \beta_1 \frac{\tau_s}{\sigma_s}\left(\frac{\epsilon}{v}\right)^{\frac{1}{2}} d_B^2 N_B \qquad (25)$$

In the analysis of floc breakup under turbulent hydrodynamic conditions, three approaches are normally employed namely: the limiting strength approach, maximum strain rate approach and the maximum floc size approach [26]. The first approach to floc breakup analysis which is based on force balances [67], requires an accurate description of the flow field in order describe the stress acting on the model floc. In this approach for analyzing the breakage phenomenon, under a given agitation condition, the critical condition of floc breakage is attained when the hydrodynamic breaking force F_H is greater than or equal to the floc binding or cohesive force F_B (B ≤ 1).

Consequently, the conceptual form of the floc growth and breakage rate mechanism can be expressed mathematically in Eqs. (26-27) while Eqs. (28-29) expressed the critical condition of floc breakage for the inertia and viscous subrange respectively [59, 59, 60, 64, 81, 116, 132-135, 140, 147]. A number of empirical models have been developed for estimating the maximum aggregate size d_{Fmax}. Few of such expressions are presented for the inertia and viscous subrange of turbulence in Table 2 [143, 144].

$$\beta_{floc} = \alpha_{ij}\beta_{col_{ij}} - \beta_{br} \qquad (26)$$

$$\beta_{floc} = (\alpha_{ijBM}\beta_{BM} + \alpha_{ijSH}\beta_{SH} + \alpha_{ijDS}\beta_{DS}) - \beta_{br}(\qquad 27)$$

$$B = \frac{Floc\ binding\ force}{Hydrodynamic\ force} = \frac{F_B}{F_h} = \frac{48^{-\frac{2}{3}}\pi^{\frac{5}{3}} d^{\frac{2}{3}} \sigma(\rho_o - \rho_w)^{\frac{2}{3}} d^{\left(1+\frac{D_f}{3}\right)}}{\frac{\pi\rho_w^2 \mu^{\frac{2}{3}} G^{\frac{4}{3}} d^{\frac{8}{3}}}{4}} \qquad (28)$$

$$B = \frac{Floc\ binding\ force}{Hydrodynamic\ force} = \frac{F_B}{F_h} = \frac{48^{-\frac{2}{3}}\pi^{\frac{5}{3}} d^{\frac{2}{3}} \sigma(\rho_o - \rho_w)^{\frac{2}{3}} d^{\left(1+\frac{D_f}{3}\right)}}{\frac{\pi\rho_w d^4 G^2}{60}} \qquad (29)$$

Table 2. Empirical and Theoretical Models for Estimating Maximum Floc Size Under Steady State Conditions

Models	Maximum floc diameter	References
1	$d_{Fmax} = K' \epsilon^{-1(1+D_p)}$	[49]
2	$d_{Fmax} = 0.68\rho^{\frac{3}{5}} d_0^{\frac{3}{5}} \epsilon^{\frac{11}{20}} v^{\frac{9}{20}} F_B^{\frac{3}{5}}$	[63][a]
3	$d_{Fmax} = \frac{6U(1-p)^{\frac{2}{3}}}{\pi^2 KG\eta d_p^2}$	[119]
4	$d_{Fmax} = \frac{(F_B/d_p)}{\rho\sqrt{\epsilon v}}$	[67, 118][b]
5	$d_{Fmax} = \left[\frac{\left(\frac{F_b}{d_P}\right)d_p^k}{\rho G v}\right]^{\frac{1}{k+1}}$	[67]*f*
5	$d_{Fmax} = \left[\frac{\left(\frac{f_B}{d_p}\right)d_p^k}{\sigma\sqrt{\epsilon v}}\right]^{\frac{1}{k+1}}$	[67]*e*
6	$d_{Fmax} = \frac{\sqrt{\frac{\sigma}{\rho_f}}}{\sqrt{\frac{\epsilon}{v}}}$	[77]*f*
7	$d_{Fmax} = \frac{\left(\frac{\sigma}{v}\right)^{\frac{1}{3}}}{\frac{1}{\epsilon}}$	[77]*e*
8	$d_{Fmax} = 2\rho^{-\frac{1}{2}}(\epsilon v)^{-\frac{1}{4}} B_f^{\frac{1}{2}}$	[35]*f*
9	$d_{Fmax} = \left[\frac{B_f v^{\frac{3}{4}}}{1.9\rho\epsilon^{\frac{11}{12}} d_p^2}\right]^{\frac{3}{5}}$	[35]*d*

[a] Inertia domain of turbulence
[b] Viscous subrange of turbulenc

The fluctuating instantaneous fluid velocities acting parallel to the surface of the floc will induce a local shear stress σ_s on the aggregate in the viscous subrange reaching a maximum value when the floc size is roughly equal to the eddy scale (Kolmogorov micro scale) [118]. Similarly, fluctuating fluid velocities normal to the floc surface or dynamic pressure fluctuations acting on opposite sides of an aggregate will results in normal or bulk pressure stress σ_t (tensile or compressive) [53]. In addition, turbulent drag forces F_D acting on the surface of an aggregate which originates from the local motion of the fluid relative to the motion of the aggregates will results in instantaneous surface shear forces and shear stress respectively [77]. It has been shown that for flocs in the inertial subrange of turbulence ($d_F > \lambda$), tensile stress will predominate causing wholesale fracture or fragmentation [35], while for those in the viscous subrange ($d_F < \lambda$), shear stress will cause erosion of the particles, floc shell or floc surface as shown schematically in Fig. 5 [47, 53].

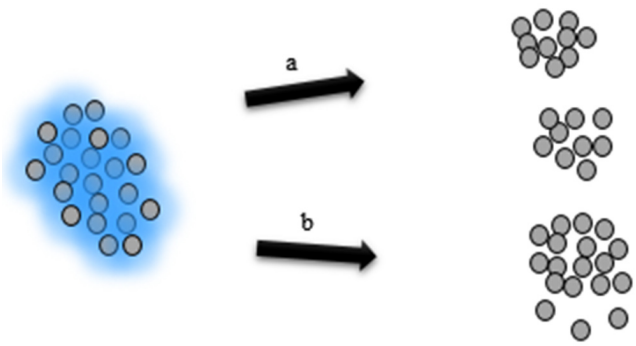

Fig. 5. Schematic representation of hydrodynamic interactions leading to floc rupture (a) floc splitting or fragmentation (b) surface erosion.

4.3. Mechanisms of Aggregate Disruption

Several mechanisms have been proposed to account for the disruption of aggregates in orthokinetic flocculation [26-28, 46, 47, 57, 67, 117, 119, 144, 146, 156-158]. In addition to floc splitting, fracture or bulk rupture and surface erosion mentioned earlier, several other mechanisms have been proposed to be responsible for floc breakage but with little experimental data or theoretical analysis. Such mechanisms include aggregate-aggregate collisions, aggregate-stirrer collisions, as well as collisions with baffles and the tank wall [35, 138].

A number of theoretical and empirical models have been developed to account for the hydrodynamic stress exerted on particle agglomerates and their cohesive strength. Considering a model floc undergoing rupture by fragmentation ($\sigma_t \geq \tau_t$) in the inertia domain of turbulence ($d_F > \lambda$), subjected to the shearing action of fluid motion, the turbulent hydrodynamic tensile stress σ_t causing bulk rupture or fragmentation by floc splitting and the aggregate tensile strength τ_t resisting the fluctuating pressure on the floc may be expressed mathematically in Eqs. (30-31).

$$\sigma_t = 0.49\rho_f(\epsilon^3 v)^{\frac{1}{4}} d_F \tag{30}$$

$$\tau_t = \frac{(1-\rho_f)B_f}{d_p^2} \tag{31}$$

Similarly, for a floc rupture due to the erosion of primary particles, micro flocs, or floc shell ($\sigma_s \geq \tau_s$) in the viscous subrange ($d_F < \lambda$); the turbulent hydrodynamic shear stress σ_s eroding the surface of the aggregates and the corresponding aggregate shear strength τ_s resisting the viscous shear forces can be expressed mathematically in Eqs. (32-33) [35].

$$\sigma_s = 0.26\rho_f(v\epsilon)^{\frac{1}{2}} \tag{32}$$

$$\tau_s = \frac{(1-\rho_f)B_f}{d_P^2} \tag{33}$$

In a related study, Mühle [67] presented floc breakup analysis on the basis of rheology. The strength of a model floc was described in terms of the surface shear yield strength τ_y resisting floc shell erosion due to pseudo-surface tension force γ_F eroding the particle chain of the outer floc surface in the viscous domain of turbulence ($\sigma_s \geq \tau_y$) (Eq. (34)). The yield stress approach was also presented by Liu et. al. [147] for calculating the maximum floc tensile yield stress σ_y at which breakage is likely to occur in the inertia subrange ($\sigma_t \geq \sigma_y$) (Eq. (35)).

$$\tau_y = \frac{F_b}{d_p^w}\left(\frac{\lambda_0}{d_F}\right)^k \tag{34}$$

$$\sigma_y = 0.5\alpha\rho\epsilon^{\frac{2}{3}}\left[\frac{2\pi}{d_f}\right]^{-\frac{2}{3}} \tag{35}$$

On a similar basis, Attia [118] presented models for predicting the critical fluid velocity V_c above which there will be floc breakage by estimating floc yield stress σ_y (tensile or compressive) resulting from dynamic pressure acting on the floc (Eqs. (36-37)). The kinetic equations for fragmentation and surface erosion mechanisms are presented in Eqs. 38-39 based on the empirical results from flocculation in stirred reactor. The quantities N_A, N_B, σ_s, τ_s, represent change in the particle number concentration per unit volume for aggregation and breakage, the aggregate shear strength and the shearing stress respectively [35, 49].

$$V_c = \sqrt{\frac{2\sigma_y}{\rho_f}} \tag{36}$$

$$\sigma_y = \frac{1}{2}\rho_f v^2 \tag{37}$$

$$-\frac{dN_A}{dt} = KN_A^2 - \beta N_B \tag{38}$$

$$\frac{dN}{dt} = \beta_1\frac{\tau_s}{\sigma_s}\left(\frac{\epsilon}{v}\right)^{\frac{1}{2}} d_f^2 N_f \tag{39}$$

4. Practical Applications and Future Outlook

Over the past decades, significant progress has been made in understanding the complex turbulent interactions that influence and drive the flocculation process. Improvement in modelling and simulation tools has led to the use of computational techniques in turbulent flow investigations. Nowadays, computational fluid dynamics provide a comprehensive information for process engineers necessary to design, optimize or retrofit various unit processes involving fluid flow as well as improving our understanding of flows in natural systems. This is extremely useful especially in investigations involving turbulent flows in devices with complex geometries with several design parameters requiring optimization without any need to perform the physical experiments [64, 136].

However, the numerical study of turbulent flow and flocculation process is still being done independently and only a few studies [159-164] deal with the integration of these interdependent processes. This is partly driven by the evolution pattern of computational fluid modelling (CFD) which was specifically developed for other industries but is now widely adopted across many fields [64]. Therefore, future studies must strive to advance research in this direction by coupling the modelling of turbulent fluid flow and aggregation processes within the computational environment in order to build on the recent progress made in these fields [64]. This in turn will assist process engineers in developing new generation of phase separation reactors more efficiently and improve our understanding and ability to accurately predict flow conditions in natural systems that are very vital for many environmental processes.

5. Conclusions

Flocculation process has been shown to be an effective particle phase separation process in engineered unit processes and is an important driver of many environmental processes (sediment transport, contaminant migration etc.) in the natural systems. The importance of hydrodynamics and flow turbulence as the main drivers of this process has been highlighted. Although significant progress has been made in the understanding of physicochemical aspects of flocculation, however, turbulence as remains a poorly understood phenomenon despite its profound influence on many engineered and life processes. This study highlights the need for closer integration of modelling and simulation tools in order to improve our understanding and ability to influence and predict these processes much more accurately.

Nomenclature

N	Particle number concentration per unit volume (m^{-3})
f_o	Orthokinetic collision efficiency (-)
f_p	Perikinetic collision efficiency (-)
r	Particle radius (m)
d, d_p	Floc or particle diameter (m)
β	Rate constant (-)
η, μ	Dynamic viscosity (Nsm^{-1})
K	Bond destruction coefficient (-)
V	Stirring vessel volume or fluid volume (m^3)
F_H	Turbulent hydrodynamic force (N)
P	Power input (W)
T_q	Shaft torque (Nm or $kgm^{-2}s^{-2}$)
N, n	Agitation speed (s^{-1}, m^{-1})
N_p	Dimensionless power number (-)
V_{tip}	Tip or tangential velocity (ms^{-1})
σ	Global hydrodynamic stress (Nm^{-1})
v	Kinematic viscosity (m2 s^{-1})
T	Absolute temperature (K)
ϵ	Mean dissipation rate of kinetic energy ($Nms^{-1}kg^{-1}$ or m^2s^{-3})
G, G	Mean velocity gradient or absolute shear rate (s^{-1})
U	Pair bonding energy (J)
$D_{F,max}$, $d_{F,max}$	Maximum floc diameter (m)
p	Flocs' porosity (-)
λ	Kolmogorov micro scale of turbulence (m)
D	Agitator or stirrer diameter (m)
R_e	Dimensionless Reynolds number (-)
ω	Angular velocity, speed or frequency ($rads^{-1}$)
pf	Fluid density (kg m^{-3})
t	Time (s)
R_x	Removal efficiency (%)
F_B	Aggregate binding or cohesive force (N)
τ	Aggregate cohesive or binding strength (Nm^{-2})

References

1. Pietsch W. Agglomeration processes: Phenomena, technologies, equipment. Weinheim: Wiley-VCH; 2002.
2. Farinato RS, Huang S-Y, Hawkins P. Polyelectrolyte-assisted dewatering. In: Farinato RS, Dubin PL, eds. Colloid-Polymer Interactions: From Fundamentals to Practice. New York (NY): John Wiley & Sons; 1993. p. 3-50.
3. Lick W. Sediment and contaminant transport in surface waters. Boca Raton (FL): CRC Press; 2008.
4. Addai-Mensah J, Prestidge CA. Structure formation in dispersed systems. In: Dobias B, Stechemesser H, eds. Coagulation and Flocculation Second: Second Edition. Boca Raton (FL): CRC Press; 2005. p. 135-216.
5. Lick W, Huang H, Jepsen R. Flocculation of fine-grained sediments due to differential settling. *J. Geophys. Res. Oceans* 1993;98:10279-10288.
6. Runkana V, Somasundaran P, Kapur PC. A population balance model for flocculation of colloidal suspensions by polymer bridging. *Chem. Eng. Sci.* 2006;61:182-191.
7. Prat OO, Ducoste JJ. Simulation of flocculation in stirred vessels lagrangian versus eulerian. *Chem. Eng. Res. Des.* 2007;85:207-219.
8. Prat OP, Ducoste JJ. Modeling spatial distribution of floc size in turbulent processes using the quadrature method of moment and computational fluid dynamics. *Chem. Eng. Sci.* 2006;61:75-86.
9. Curran SJ, Black RA. Taylor-vortex bioreactors for enhanced mass transport. In: Chaudhuri J, Al-Rubeai M, eds. Bioreactors for tissue engineering: Principles, design and operation. dordrecht: Springer; 2005. p. 47-85.
10. Wu W. Computational river dynamics. London: CRC Press; 2008.
11. Sievers M, Stoll SM, Schroeder C, et al. Sludge dewatering and aggregate formation effects through taylor vortex assisted flocculation. *Sep. Sci. Technol.* 2008;43:1595-1609.
12. Tooby PF, Wick GL, Isaacs JD. The motion of a small sphere in a rotating velocity field: A possible mechanism for suspending particles in turbulence. *J. Geophys. Res.* 1977;82:2096-2100.

13. Taboada-Serrano P, Chin C-J, Yiacoumi S, Tsouris C. Modeling aggregation of colloidal particles. *Curr. Opin. Colloid Interface Sci.* 2005;10:123-132.
14. Biggs S. Aggregate structures and solid-liquid separation processes. *KONA Powder Part J* 2006;24:41-53.
15. Gregory J, Guibai L. Effects of dosing and mixing conditions on polymer flocculation of concentrated suspensions. *Chem. Eng. Commun.* 1991;108:3-21.
16. Yukselen MA, Gregory J. The effect of rapid mixing on the break-up and re-formation of flocs. *J. Chem. Technol. Biotechnol.* 2004;79:782-788.
17. Lee KE, Morad N, Teng TT, Poh BT. Development, characterization and the application of hybrid materials in coagulation/flocculation of wastewater: A review. *Chem. Eng. J.* 2012;203:370-386.
18. Hjorth M, Christensen ML. Evaluation of methods to determine flocculation procedure for manure separation. *Trans ASABE* 2008;51:2093-2103.
19. Logan BE. Environmental transport processes. Hoboken (NJ): John Wiley & Sons; 2012.
20. Milligan TG, Hill PS. A laboratory assessment of the relative importance of turbulence, particle composition, and concentration in limiting maximal floc size and settling behaviour. *J. Sea Res.* 1998;39:227-241.
21. Gregory J. Fundamentals of flocculation. *Crit. Rev. Environ. Control* 1989;19:185-230.
22. Popa I, Papastavrou G, Borkovec M. Charge regulation effects on electrostatic patch-charge attraction induced by adsorbed dendrimers. *Phys. Chemsitry Chem. Phys.* 2010;12:4863-4871.
23. Gregory J. The role of colloid interactions in solid-liquid separation. *Water Sci. Technol.* 1993;27:1-17.
24. Bratby J. Coagulation and flocculation in water and wastewater treatment. London: IWA Publishing; 2006.
25. Bache DH, Gregory R. Flocs in water treatment. London: IWA Publishing; 2007.
26. Benjamin MM, Lawler DF. Water quality engineering: Physical/chemical treatment processes. Hoboken (NJ): John Wiley & Sons; 2013.
27. Partheniades E. Cohesive sediments in open channels: Properties, transport and applications. Oxford: Butterworth-Heinemann; 2009.
28. Gregory J. Particles in water: Properties and processes. Boca Raton (FL): CRC Press; 2006.
29. Shammas NK. Coagulation and flocculation. In: Wang LK, Hung Y-T, Shammas NK, eds. Physicochemical Treatment Processes. Totowa (NJ): Humana Press; 2005. p. 103-139.
30. Marshall JS, Li S. Adhesive particle flow: A discrete-element approach. New York (NY): Cambridge University Press; 2014.
31. Lebovka NI. Aggregation of charged colloidal particles. In: Müller M, ed. Polyelectrolyte complexes in the dispersed and solid state I. Heidelberg: Springer; 2013. p. 57-96.
32. Nopens I. Modelling the activated sludge flocculation process: A population balance approach [dissertation]. Ghent: Univ. of Ghent; 2005.
33. Moody G, Norman P. Chemical pre-treatment. In: Tarleton S, Wakeman R, eds. Solid-Liquid Separation: Scale-up of industrial equipment. Oxford: Elsevier; 2005. p. 38-81.
34. Laskowski JS, Pugh RJ. Dispersions stability and dispersing agents. In: Laskowski JS, Ralston J, eds. Colloid chemistry in mineral processing. Amsterdam: Elsevier; 1992. p. 115-170.
35. Lu S, Ding Y, Guo J. Kinetics of fine particle aggregation in turbulence. *Adv. Colloid. Interface Sci.* 1998;78:197-235.
36. Wilkinson KJ, Reinhardt A. Contrasting roles of natural organic matter on colloidal stabilization and flocculation. In: Liss SN, Droppo IG, Leppard GG, Milligan TG, eds. Flocculation in Natural and Engineered Environmental Systems. Boca Raton (FL): CRC Press; 2005. p. 143-170.
37. Bagster DF. Aggregate behaviour in stirred vessels. In: Shamlou AP, ed. Processing of solid-liquid suspensions. Oxford: Butterworth-Heinemann; 1993. p. 26-58.
38. Smith-Palmer T, Pelton R. Flocculation of particles. In: Somasundaran P, ed. Encyclopedia of Surface and Colloidal Science. 5th ed. Boca Raton (FL): CRC Press; 2006. p. 2584-2599.
39. Schramm LL. Emulsions, foams, and suspensions. Weinheim: Wiley VCH; 2005.
40. Gregory J. Stability and flocculation of suspensions. In: Shamlou AP, ed. Process. Solid-Liquid Suspensions. Oxford: Butterworth-Heinemann; 1993. p. 59-92.
41. Grasso D, Subramaniam K, Butkus M, et al. A review of non-dlvo interactions in environmental colloidal systems. *Rev. Environ. Sci. Biotechnol.* 2002;1:17-38.
42. Gregory J. Flocculation of fine particles. In: Mavros P, Matis KA, eds. Innovations in floatation technology. Dordrecht: Springer; 1992. p. 101-124.
43. Hanson AT, Cleasby JL. The effects of temperature on turbulent flocculation: Fluid dynamics and chemistry. *J. Am. Water Works Assoc.* 1990;82:56-73.
44. Kissa E. Dispersions: Characterization, testing, and measurement. New York (NY): Marcel Dekker; 1999.
45. Gregory J. Flocculation fundamentals. In: Tadros T, ed. Encyclopedia of colloid and interface science. Heidelberg: Springer; 2013. p. 459-491.
46. Van Leussen W. Aggregation of particles, settling velocity of mud flocs-a review. In: Dronkers J, Van Leussen W, eds. Physical processes in estuaries. Heidelberg: Springer; 2011. p. 347-403.
47. Thomas DN, Judd SJ, Fawcett N. Flocculation modelling: A review. *Water Res.* 1999;33:1579-1592.
48. Atkinson JF, Chakraborti RK, Benschoten JE. Effects of floc size and shape in particle aggregation. In: Liss SN, Droppo IG, Leppard GG, Milligan TG (eds) Flocculation in natural and engineered environmental systems. Boca Raton (FL): CRC Press; 2005. p. 95-120.
49. Kramer TA, Clark MM. Incorporation of aggregate breakup in the simulation of orthokinetic coagulation. *J. Colloid Interface Sci.* 1999;216:116-126.
50. Lick W, Lick J, Ziegler CK. Flocculation and its effect of the vertical transport of fine-grained sediments. In: Hart BT, Sly PG, eds. Sediment/Water Interactions. Heidelberg: Springer; 1992. p. 1-16.
51. Lick W, Lick J, Ziegler CK. Flocculation and its effect of the vertical transport of fine-grained sediments. *Hydrobiologia* 1992;235-236:1-16.

52. Lawler FD. Physical aspects of flocculation: From microscale to macroscale. *Water Res.* 1993;27:165-180.
53. Kruster KA. The influence of turbulence on aggregation of small particles in agitated vessels [dissertation]. Eindhoven: Technical Univ. Eindhoven; 1991.
54. Lick W, Lick J. Aggregation and disaggregation of fine-grained lake sediments. *J. Gt. Lakes Res.* 1998;14:514-523.
55. Tsai C-H, Iacobellis S, Lick W. Flocculation of fine-grained lake sediments due to a uniform shear stress. *J. Gt. Lakes Res.* 1987;13:135-146.
56. Wang L, Marchisio DL, Vigil RD, Fox RO. CFD simulation of aggregation and breakage processes in laminar taylor-couette flow. *J. Colloid Interface Sci.* 2005;282:380-396.
57. Gregory J. Floc formation and floc structure. In: Newcombe G, Dixon D, eds. Interface science in drinking water treatment: Theory and applications. London: Academic Press; 2006. p. 25-43.
58. Letterman RD, Amirtharajah A, O'Meila CR. Coagulation and flocculation. In: Edzwald J, ed. Water Quality & Treatment: A Handbook on Drinking Water. New York (NY): McGraw-Hill; 2010. p. 6.1-6.66.
59. Bridgeman J, Jefferson B, Parsons SA. The development and application of CFD models for water treatment flocculators. *Adv. Eng. Softw.* 2010;41:99-109.
60. Bridgeman J, Jefferson B, Parsons S. Assessing floc strength using CFD to improve organics removal. *Chem. Eng. Res. Des.* 2008;86:941-950.
61. Camp TR, Stein PC. Velocity gradients and internal work in fluid motion. *J. Boston Soc. Civ. Eng.* 1943;30:219-237.
62. Winterwerp JC. A simple model for turbulence induced flocculation of cohesive sediment. *J. Hydraul Res.* 1998;36:309-326.
63. Zhu Z. Theory on orthokinetic flocculation of cohesive sediment: A review. *J. Geosci. Environ. Prot.* 2014;2:13-23.
64. Bridgeman J, Jefferson B, Parsons SA. Computational fluid dynamics modelling of flocculation in water treatment: A review. *Eng Appl. Comput. Fluid Mech.* 2009;3:220-241.
65. Korpijärvi J, Laine E, Ahlstedt H. Using CFD in the study of mixing in coagulation and flocculation. In: Hahn HH, Hoffmann E, Odegaard H (eds) Chemical Water Wastewater Treatment VI. Heidelberg: Springer; 2000. p. 89-99.
66. Kramer TA, Clark MM. Influence of strain-rate on coagulation kinetics. *J. Environ. Eng.* 1997;123:444-452.
67. Mühle K. Floc stability in laminar and turbulent flow. In: Dobias B, ed. Coagulation and Flocculation: Theory and Applications. New York (NY): Marcel Dekker; p. 355-390.
68. Svarovsky L. Solid-liquid separation. 4th ed. Woburn, MA: Butterworth-Heinemann; 2000.
69. Ives KJ. Experiments in orthokinetic flocculation. In: Gregory J, ed. Solid-Liquid Separation. London: Ellis Horwood Ltd; 1984. p. 196-220.
70. Belfort G (1986) Fluid mechanics and cross-flow membrane filtration. In: Muralidhara HS, ed. Advances in Solid-Liquid Separation. Columbus (OH): Battelle Press; 1986. p. 165-189.
71. Spicer PT. Shear-induced aggregation-fragmentation: Mixing and aggregate morphology effects [dissertation]. Cincinnati: Univ. of Cincinnati; 1997.
72. Falk L, Commenge J. Characterization of mixing and segregation in homogeneous flow systems. In: Hessel V, Renken A, Schouten JC, Yoshida J, eds. Handbook of Micro Reactors. Weinheim: John Wiley & Sons; 2009. p. 147-171.
73. Concha F. Solid-liquid separation in the mining industry. Heidelberg: Springer; 2014.
74. Farrow JB, Swift JD. A new procedure for assessing the performance of flocculants. Int. *J. Miner Process* 1996;46:263-275.
75. Carissimi E, Rubio J. Polymer-bridging flocculation performance using turbulent pipe flow. *Miner Eng.* 2015;70:20-25.
76. Hendricks DW. Fundamentals of water treatment unit processes: Physical, chemical, and biological. Boca Raton (FL): CRC Press; 2011.
77. Shamlou AP, Hooker-Titchener N. Turbulent aggregation and breakup of particles in liquids in stirred vessels. In: Shamlou AP, ed. Processing of solid-liquid suspensions. Oxford: Butterworth-Heinemann; 1993. p. 1-25.
78. Hogg R. Flocculation and dewatering. *Int. J. Miner Process* 2000;58:223-236.
79. Bergenstahl B. Emulsions. In: Beckett ST, ed. Physico-chemical aspects of food processing. glasgow: Blackie Academic & Professional; 1995. p. 49-64.
80. Son M, Hsu T. Flocculation model of cohesive sediment using variable fractal dimension. *Environ. Fluid Mech.* 2008;8:55-71.
81. Adachi Y, Kobayashi A, Kobayashi M. Structure of colloidal flocs in relation to the dynamic properties of unstable suspension. *Int. J. Polym Sci.* 2012;1-14.
82. Tambo N. Optimization of flocculation in connection with various solid-liquid separation processes. In: Hahn H, Klute R, eds. Chemical water wastewater treatment. Heidelberg: Springer; 1990. p. 17-32.
83. Yusa M, Suzuki H, Tanaka S. Separating liquids from solids by pellet flocculation. *J. Am. Water Works Assoc.* 1975;67: 397-402.
84. Yusa M, Igarashi C. Compaction of flocculated material. *Water Res.* 1984;18:811-816.
85. Higashitani K, Shibata T, Matsuno Y. Formation of pellet flocs from kaolin suspension and their properties. *J. Chem. Eng. Jpn.* 1987;20:152-157.
86. Yusa M, Gaudin AM. Formation of pellet-like flocs of kaolinite by polymer chains. *Am. Ceram Soc. Bull.* 1964;43:402-406.
87. Yusa M. Mechanisms of pelleting flocculation. *Int. J. Miner Process* 1977;4:293-305.
88. Wang X, Jin P, Yuan H, et al. Pilot study of a fluidized-pellet-bed technique for simultaneous solid/liquid separation and sludge thickening in a sewage treatment plant. *Water Sci. Technol.* 2004;49:81-88.
89. Gang Z, Ting-lin H, Chi T, et al. Settling behaviour of pellet flocs in pelleting flocculation process: Analysis through operational conditions. *Water Sci. Technol.* 2010;62:1346-1352.
90. Bähr S. Experimental studies of fundamental processes of pelleting flocculation [dissertation]. Cottbus: Brandenburg Univ. of Technology; 2006.
91. Walaszek W. Investigation upon structure of pellet flocs against process performance as a tool to optimize sludge conditioning [dissertation]. Cottbus: Brandenburg Univ. of Technology; 2007.
92. Panswad T, Polwanich S. Pilot plant application of pellet-

isation process on low-turbidity river water. *J. Water Supply Res. Technol-AQUA* 1998;47:236-244.
93. Glasgow L. Physicochemical influences upon floc deformability, density, and permeability. In: 7th world congress of chemical engineering; 2005 Jul 10-14; Glasgow, Scotland.
94. Gillberg L, Hanse B, Karlsson I, et al. About water treatment., Helsingborg: Kemira Kemwater; 2003.
95. Yusa M. Pelleting flocculation in sludge conditioning - An overview. In: Attia YA, ed. Flocculation in Biotechnology and Separation Systems. Amsterdam: Elsevier; 1987. p. 755-763.
96. Hemme A, Polte R, Ay P. Pelleting flocculation: The alternative to traditional sludge conditioning. *Aufbereit-Tech* 1995;36:226-235.
97. Amirtharajah A, Tambo N. Mixing in water treatment. In: Amirtharajah A, Clark MM, Trussell R, eds. Mixing in Coagulation and Flocculation. Denver (CO): American Water Works Association; 1991. p. 3-34.
98. Higashitani K, Kubota T. Pelleting flocculation of colloidal latex particles. *Powder Technol.* 1987;51:61-69.
99. Vigdergauz VE, Gol'berg GY. Kinetics of mechanical floccule synaeresis. *J. Min. Sci.* 2012;48:347-353.
100. Walaszek W, Ay P. Extended interpretation of the structural attributes of pellet flocs in pelleting flocculation. *Miner Eng.* 2006;19:1397-1400.
101. Walaszek W, Ay P. Porosity and interior structure analysis of pellet-flocs. *Colloids Surf. Physicochem Eng. Asp.* 2006;280: 155-162.
102. Walaszek W, Ay P. Pelleting flocculation: An alternative technique to optimise sludge conditioning. *Int. J. Miner Process* 2005;76:173-180.
103. Tambo N, Wang CC. The mechanism of pellet flocculation in fluidized-bed operations. *J. Water Supply Res. Technol-AQUA* 1993;42:67-76.
104. Hjorth M. Flocculation and solid-liquid separation of animal slurry: Fundamentals, control and application [dissertation]. Odense: Univ. of Southern Denmark; 2009.
105. Wang XH, Jiang C. Papermaking part II: Surface and colloid chemsitry of papermaking process. In: Somasundaran P, ed. Encyclopedia of Surface and Colloid Science. 5th ed. Boca Raton (FL): CRC Press; 2006. p. 4435-4451.
106. Xiao H. Fine clay flocculation. In: Somasundaran P, ed. Encyclopedia of surface and colloid science. 5th ed. Boca Raton (FL): CRC Press; 2006. p. 2572-2583.
107. Petzold G, Schwarz S. Polyelectrolyte complexes in flocculation applications. In: Müller M, ed. Polyelectrolyte complexes in the dispersed and solid state II. Heidelberg: Springer; 2013. p. 25-65.
108. Moudgil BM. Selection of flocculants for solid-liquid separation process. In: Muralidhara HS, ed. Advances in solid-liquid separation. Columbus (OH): Battelle Press; 1986. p. 191-204.
109. Böhm N, Kulicke W-M. Optimization of the use of polyelectrolytes for dewatering industrial sludges of various origins. *Colloid Polym. Sci.* 1997;275:73-81.
110. Besra L, Sengupta DK, Roy SK, Ay P. Polymer adsorption: Its correlation with flocculation and dewatering of kaolin suspension in the presence and absence of surfactants. *Int. J. Miner Process* 2002;66:183-202.
111. Hjorth M, Christensen ML, Christensen PV. Flocculation, coagulation, and precipitation of manure affecting three separation techniques. *Bioresour Technol.* 2008;99:8598-8604.
112. Hjorth M, Jørgensen BU. Polymer flocculation mechanism in animal slurry established by charge neutralization. *Water Res.* 2012;46:1045-1051.
113. Lee CH, Liu JC. Enhanced sludge dewatering by dual polyelectrolytes conditioning. *Water Res.* 2000;34:4430-436.
114. Lagaly G. From clay mineral crystals to colloidal clay mineral dispersions. In: Dobias B, ed. Coagulation and flocculation: Theory and applications. New York (NY): Marcel Dekker; 1993. p. 427-494.
115. Lagaly G. From clay mineral crystals to colloidal clay mineral dispersions. In: Dobias B, Stechemesser H, eds. Coagulation and flocculation: Second Edition. Boca Raton (FL): CRC Press; 2005. p. 519-600.
116. Coufort C, Bouyer D, Liné A. Flocculation related to local hydrodynamics in a taylor-couette reactor and in a jar. *Chem. Eng. Sci.* 2005;60:2179-2192.
117. Boyle JF, Manas-Zloczower I, Feke DL. Hydrodynamic analysis of the mechanisms of agglomerate dispersion. *Powder. Technol.* 2005;153:127-133.
118. Attia YA. Flocculation. In: Laskowski JS, Ralston J, eds. Colloid chemistry in mineral processing. Amsterdam: Elsevier; 1992. p. 277-308.
119. Rulyov NN. Physicochemical microhydrodynamics of ultradisperse systems. In: Starov VM, ed. Nanoscience: Colloidal and Interfacial Aspects. Boca Raton (FL): CRC Press; 2010. p. 969-995.
120. Zlokarnik M. Stirring: Theory and practice. Weinheim: Wiley-VCH; 2008.
121. Baldyga J, Bourne JR. A fluid mechanical approach to turbulent mixing and chemical reaction part II micromixing in the light of turbulence theory. *Chem. Eng. Commun.* 1984;28: 243-258.
122. Thomas SF, Rooks P, Rudin F, et al. Swirl flow bioreactor containing dendritic copper-containing alginate beads: A potential rapid method for the eradication of escherichia coli from waste water streams. *J. Water Process Eng.* 2015;5:6-14.
123. Kresta SM, Brodkey RS. Turbulence in mixing applications. In: Paul EL, Atiemo-Obeng VA, Kresta SM, eds. Handbook of Industrial Mixing: Science and Practice. Hoboken (NJ): John Wiley & Sons; 2004. p. 19-87.
124. Thoenes D. Chemical reactor development: From laboratory synthesis to industrial production. Dordrecht: Springer; 1998.
125. Sparks T. Fluid mixing in rotor/stator mixers [dissertation]. Cranfield: Cranfield Univ.; 1996.
126. Bałdyga J, Pohorecki R. Turbulent micromixing in chemical reactors: A review. *Chem. Eng. J. Biochem. Eng.* 1995;58:183-195.
127. Oldshue JY, Trussell RR. Design of impellers for mixing. In: Amirtharajah A, Clark MM, Trussell R, eds. Mixing in coagulation and flocculation. Denver (CO): American water works association; 1991. p. 309-342.
128. Kockmann N. Transport phenomena in micro process engineering. Heidelberg: Springer; 2008.
129. Maggi F. Flocculation dynamics of cohesive sediment

[dissertation]. Delft: Delft Univ. of Technology; 2005.
130. Bałdyga J, Bourne JR. Turbulent mixing and chemical reactions. Weinheim: Wiley-VCH; 1999.
131. Wu H, Patterson GK. Laser-doppler measurements of turbulent-flow parameters in a stirred mixer. *Chem. Eng. Sci.* 1989;44:2207-2221.
132. Kobayashi M, Adachi Y, Ooi S. Breakup of fractal flocs in a turbulent flow. *Langmuir* 1999;15:4351-4356.
133. Bouyer D, Liné A, Do-Quang Z. Experimental analysis of floc size distribution under different hydrodynamics in a mixing tank. *AIChE J.* 2004;50:2064-2081.
134. Bouyer D, Coufort C, Liné A, Do-Quang Z. Experimental analysis of floc size distributions in a 1-L jar under different hydrodynamics and physicochemical conditions. *J. Colloid Interface Sci.* 2005;292:413-428.
135. He J, Liu J, Yuan Y, Zhang J. A novel quantitative method for evaluating floc strength under turbulent flow conditions. *Desalination Water Treat.* 2014;56:1975-1984.
136. Argyropoulos CD, Markatos NC. Recent advances on the numerical modelling of turbulent flows. *Appl. Math Model* 2015;39:693-732.
137. Bubakova P, Pivokonsky M, Filip P. Effect of shear rate on aggregate size and structure in the process of aggregation and at steady state. *Powder Technol.* 2013;235:540-549.
138. Bemmer GG. Agglomeration in suspension: A study of mechanisms and kinetics [dissertation]. Delft: Delft Univ. of Technology; 1979.
139. Spicer PT, Pratsinis SE. Shear-induced flocculation: The evolution of floc structure and the shape of the size distribution at steady state. *Water Res.* 1996;30:1049-1056.
140. Soos M, Moussa AS, Ehrl L, et al. Effect of shear rate on aggregate size and morphology investigated under turbulent conditions in stirred tank. *J. Colloid Interface Sci.* 2008;319: 577-589.
141. Carissimi E, Rubio J. The flocs generator reactor-fgr: A new basis for flocculation and solid-liquid separation. *Int. J. Miner Process* 2005;75:237-247.
142. Carissimi E, Miller JD, Rubio J. Characterization of the high kinetic energy dissipation of the flocs generator reactor (FGR). *Int. J. Miner Process* 2007;85:41-49.
143. Yuan Y, Farnood RR. Strength and breakage of activated sludge flocs. *Powder Technol.* 2010;199:111-119.
144. Jarvis P, Jefferson B, Gregory J, Parsons SA. A review of floc strength and breakage. *Water Res.* 2005;39:3121-3137.
145. Tambo N, François RJ. Mixing, breakup and floc characteristics. In: Amirtharajah A, Clark MM, Trussell R, eds. Mixing in Coagulation and Flocculation. Denver (CO): American Water Works Association; 1991. p. 256-281.
146. Yeung AKC, Pelton R. Micromechanics: A new approach to studying the strength and breakup of flocs. *J. Colloid Interface Sci.* 1996;184:579-585.
147. Liu SX, Glasgow LA. Aggregate disintegration in turbulent jets. *Water Air Soil Pollut.* 1997;95:257-275.
148. Glasgow LA, Liu X. Response of aggregate structures to hydrodynamic stress. *AIChE J.* 1991;37:1411-1414.
149. Wang G, Zhou S, Joshi JB, et al. An energy model on particle detachment in the turbulent field. *Miner Eng.* 2014;69:165-169.
150. Bache DH. Floc rupture and turbulence: A framework for analysis. *Chem. Eng. Sci.* 2004;59:2521-2534.
151. Partheniades E. Turbulence, flocculation and cohesive sediment dynamics. In: Mehta AJ, ed. Nearshore and estuarine cohesive sediment transport. Washington DC: American Geophysical Union; 1993. p. 40-59.
152. Hogg R. Flocculation and dewatering of fine-particle suspension. In: Dobias B, Stechemesser H, eds. Coagulation and flocculation: Second Edition (FL): CRC Press, Boca Raton; 2005. p. 805-850.
153. Serra T, Casamitjana X. Modelling the aggregation and break-up of fractal aggregates in a shear flow. *Appl. Sci. Res* 1997;59:255-268.
154. McConnachie G. Turbulence intensity of mixing in relation to flocculation. *J. Environ. Eng.* 1991;117:731-750.
155. Haralampides K, McCorquodale AJ, Krishnappan BG. Deposition properties of fine sediment. *J. Hydraul Eng.* 2003;129:230-234.
156. Dobias B, Von Rybinski W. Stability of dispersions. In: Dobias B, Qiu X, Von Rybinski W, eds. Solid-liquid dispersions. New York (NY): Marcel Dekker; 1999. p 244-278.
157. Peng SJ, Williams RA. Control and optimisation of mineral flocculation and transport processes using on-line particle size analysis. *Miner Eng.* 1993;6:133-153.
158. Neumann LE, Howes T. Aggregation and breakage rates in the flocculation of estuarine cohesive sediments. In: Maa JPY, Sanford LP, Schoellhamer DH, eds. Estuarine and coastal fine sediment dynamics. Amsterdam: Elsevier; 2007. p. 35-53.
159. Oshinowo L, Elsaadawy E, Vilagines R. CFD modeling of oil-water separation efficiency in three-phase separators. In: 10th International Conference on Computational Fluid Dynamics in the Oil & Gas, Metallurgical and Process Industries; 2014 Jun 17-19; Trondheim, Norway. Oslo: SINTEF Academic Press; 2015. p. 207-216.
160. Nopens I. Improved prediction of effluent suspended solids in clarifiers through integration of a population balance model. In: IWA Particle Separation Conference; 2007 Jul 9-12; Toulouse, France.
161. Heath AR, Koh PTL. Combined population balance and CFD modelling of particle aggregation by polymeric flocculant. In: 3rd International Conference on CFD in the Minerals and Process Industries; 2003 Dec 10-12; Melbourne, Australia. p. 339-344.
162. Torfs E. Different settling regimes in secondary settling tanks: Experimental process analysis, model development and calibration [dissertation]. Ghent: Ghent Univ.; 2015.
163. Torfs E, Vesvikar M, Nopens I. Improved predictions of effl uent suspended solids in wastewater treatment plants by integration of a PBM with computational fluid dynamics. In: 5th population balance modelling conference; 2013 Sep 11-13; Bangalore, India.
164. Lee BJ, Molz F. Numerical simulation of turbulence-induced flocculation and sedimentation in a flocculant-aided sediment retention pond. *Env. Eng. Re.s* 2014;19:165-174.